DRIFTING-SNOW SIMILITUDE—TRANSPORT-RATE AND ROUGHNESS MODELING

By J. D. IVERSEN

(Department of Aerospace Engineering, Iowa State University, Ames, Iowa 50010, U.S.A.)

ABSTRACT. This paper reports on results from a series of experiments in a boundary-layer wind tunnel concerning snow-drift control adjacent to grade separations on interstate highways. A new application of similitude principles making use of theoretical relationships involving drifting particulate material is presented. The primary modeling parameters are considered to be a mass-rate parameter and an aerodynamic roughness parameter. They are derived by considerations of mass-transport rate of material in saltation and the equivalent roughness height of material in saltation. The parameters are combined empirically to correlate model snow-drift data successfully as well as to predict equivalent full-scale wind speeds and storm durations. The combined parameter has been used to compare and evaluate a variety of drift-control techniques adjacent to an interstate highway grade-separation crossing.

RÉSUMÉ. *Simulation du chasse-neige: modélisation de la vitesse de transport et de la rugosité.* Cet article se rapporte aux résultats d'une série d'expériences dans un tunnel d'étude de la couche limite du vent destiné à contrôler le chasse-neige dans un croisement à deux niveaux d'autoroutes interétats. On présente une nouvelle application des principes de similitude faisant usage des relations théoriques concernant le matériel particulier prenant part au chasse-neige. On considère que les paramètres principaux de la similitude sont un paramètre de débit et un paramètre de rugosité aérodynamique. Ils sont obtenus à partir de considérations de vitesse de transport de masse du matériel en saltation et de la hauteur équivalente de rugosité du matériel en saltation. Les paramètres sont combinés empiriquement pour obtenir une bonne corrélation des données du chasse-neige sur le modèle ainsi que pour prédire les équivalents en vraie grandeur des vitesses du vent et de la durée des tempêtes de neige. Le paramètre combiné a été utilisé pour comparer et évaluer diverses techniques du contrôle du chasse-neige au voisinage d'un croisement d'autoroutes à deux niveaux.

ZUSAMMENFASSUNG. *Modellversuche zur Schneedrift — Transportgeschwindigkeit und Rauhigkeit.* Die Arbeit berichtet über Ergebnisse aus einer Versuchsreihe in einem Grenzschicht-Windkanal, die der Erfassung der Schneedrift an Überführungen von Fernstrassen galten. Es wird eine neue Anwendung von Modellierungsprinzipien dargestellt, die theoretische Beziehungen bezüglich des driftenden Teilchenmaterials benutzt. Als Hauptparameter des Modells werden ein Parameter der Massenmenge und einer der aerodynamischen Rauhigkeit betrachtet. Sie werden aus Betrachtungen der Transportgeschwindigkeit des verwirbelten Materials und seiner äquivalenten Rauhigkeitshöhe hergeleitet. Die Parameter werden empirisch mit Erfolg zur Korrelation von Daten des Schneedriftmodells wie auch zur Vorhersage der äquivalenten Gesamtgeschwindigkeit des Windes und zur Auswertung einer Reihe von Techniken zur Driftverhinderung an einer Fernstrassenüberführung herangezogen.

LIST OF SYMBOLS

A	Planform drift area, m^2
A_c	Longitudinal drift cross-section area, m^2
A_I	Threshold speed coefficient, $u_{*t}(\rho/\rho_p g D_p)^{\frac{1}{2}}$
C_D	Drag coefficient
D_p	Particle diameter, μm
e	Coefficient of restitution
g	Gravitational acceleration, m/s^2
H	Characteristic vertical dimension, m
h	All other vertical dimensions, m
L	Characteristic horizontal dimension, m
l	All other horizontal dimensions, m
$L^{\star}$	Monin–Obhukov stability length, m
q_s	Mass-transport rate, kg/s
t	Time, s
u	Wind speed, m/s
u_*	Surface friction speed, m/s
u_{*t}	Threshold friction speed, m/s
U	Reference wind-speed (for this study, the speed at bridge height, $0.9U_\infty$ for Model 1 and $0.95U_\infty$ for Model 2), m/s

393

U_∞ Wind-tunnel free-stream speed (above boundary layer), m/s
U_0 Free-stream or reference wind-speed at initiation of motion (threshold), m/s
U_F Particle terminal speed, m/s
V Drift volume, m³
z_0 Aerodynamic roughness height, m
z_0' Aerodynamic roughness height in saltation, m
λ Ripple wave length, m
ν Kinematic viscosity, m²/s
ρ Fluid density, kg/m³
ρ_p Particle density, kg/m³

INTRODUCTION

This paper reports on results from a series of experiments conducted by the author concerning snow-drift control adjacent to grade separations (bridge overpasses) on interstate highways. This work was supported by the Iowa State Department of Transportation, with the approval and recommendation of the Iowa Highway Research Board, and by the Engineering Research Institute of Iowa State University.

A number of scale-model studies have been carried out in an attempt to determine full-scale snow-drifting phenomena. Experiments that have been conducted in water include those of Norem (1974), Isyumov (1971), Calkins (1975), de Krasinski and Anson (1975), and Theakston (1970). Wind-tunnel experiments have been conducted by Finney (1934, 1937, 1939), Nøkkentved (1940), Becker (1944), Gerdel and Strom (1961), Strom and others (1962), and Brier (1972). Tabler (1980) has conducted scale-model experiments in the atmosphere using actual snow as the modeling material. Some of these experiments have attempted to satisfy similitude requirements, at least partially. In others, modeling laws have been ignored. The current experiments demonstrate the utility of a new application of similitude fundamentals which makes use of theoretical relationships for mass-transport rate and aerodynamic roughness of saltating particulate material.

SIMILITUDE LAWS

If simple dimensional analysis is used to group the important variables involved in drifting phenomena, the following list of dimensionless parameters can be written:

1.	D_p/L	Particle diameter–length ratio
2.	$u(H)/U_F$	Reference-to-particle terminal speed ratio
3.	$[u(H)]^2/gL$	Froude number
4.	e	Coefficient of restitution
5.	$l/L, h/H$	Topographic geometric similarity
6.	z_0/L	Roughness similitude
7.	z_0'/L	Roughness similitude in saltation
8.	H/L	Reference height ratio
9.	$z_0/L^\star$	Stability parameter
10.	λ/L	Ripple length ratio
11.	$U_F/u_{\ast t}$	Particle property similitude
12.	$u_{\ast t}D_p/\nu$	Particle friction Reynolds number
13.	$u(H) L/\nu$	Flow Reynolds number
14.	$u_\ast/u_{\ast t}$	Friction speed ratio
15.	ρ/ρ_p	Density ratio
16.	$u(H) t/L$	Time scale

It is impossible, of course, in a small-scale model to satisfy all of these parameters simultaneously. Gerdel and Strom (1961) considered the parameters 1 to 4 of the foregoing list as those of primary importance. Odar (1965) and Kind (1976) have also studied the problem in some detail. The parameters considered important by these and other investigators are listed in Table I. These dimensionless quantities have been discussed previously by the author (Iversen, 1979, unpublished; Iversen and others, 1973, 1975, 1976; Ring and others, 1979).

TABLE I. MODELING PARAMETERS CONSIDERED BY VARIOUS INVESTIGATORS

Parameter No.	Gerdel and Strom (1961)	de Krasinki and Anson (1975)	Odar	Calkins	Norem	Kind	Isyumov
1	*	*			*		*
2	*	*		*	*	*	*
3	*	*	*	*	*	*	*
4	*	*					
7						*	
11				*	*	*	
12	*		*	*			*
13		*					
14			*	*			
15	*	*	*				*
3×15			*	*			
3×15/1	*	*	*		*		

Obviously, there is some disagreement as to which similitude parameters are significant. The most popular parameter is the Froude number, parameter number 3, chosen by all seven investigators as appropriate for similitude. That the Froude number by itself is not an appropriate parameter is shown by the results of the current investigation.

As shown previously (Iversen and others, 1976; Iversen, 1979), combinations of some of the similitude parameters can be obtained by using theoretical relationships. The particle trajectory equations of motion are used to group parameters 1, 3, 8, and 15 to obtain

17. $$C_D \rho L / \rho_p D_p,$$

18. $$gL^2 / u_*^2 H.$$

The equivalent roughness height in saltation z_0' is assumed to be proportional to $\rho u_*^2 / \rho_p g$ (instead of u_*^2 / g as assumed by Owen (1964)) in order to account for the effects of particle-to-fluid density ratio (White and others, 1976). Thus (Iversen and others, 1976; Iversen, 1979)

19. $$z_0'/H \approx \rho u_*^2 / \rho_p g H \approx A_1^2 (D_p/H)(u_*/u_{*t})^2.$$

A modification of Bagnold's (1941) mass transport rate,

$$q_s \approx \frac{\rho u_*^2}{g} (u_* - u_{*t}),$$

is used to obtain a transport-rate similitude parameter (Iversen, unpublished)

20. $$\frac{d(A/L^2)}{d(u_{*t}/L)} \bigg/ \left\{ \left(\frac{\rho}{\rho_p}\right) \frac{u_*^2}{gH} \left(1 - \frac{u_{*t}}{u_*}\right) \right\}.$$

Here A is the planform drift area. The differential $d(A/L^2)$ can be replaced by $d(A_c/LH)$ (cross-section area) or by $d(V/L^2H)$ (drift volume).

Odar (1962, 1965) and Kind (1976) have used theoretical aids in order to group modeling parameters or to determine important variables. Odar also considered the dimensionless particle equations of motion. In one case (Odar, 1965) he defines the dimensionless time as $t(g/L)^{\frac{1}{2}}$ rather than tU/L and instead of parameters 17 and 18 his resulting parameters are $C_D \rho u_*^2 / \rho_p g D_p$ and gL/u_*^2. In the other case (Odar, 1962) he lists the two parameters $\rho_p g L / \rho u_*^2$ and gL/u_*^2 as the important ones resulting from the particle equations of motion.

Kind (1976) also considers the equivalent roughness height z_0' to be important in modeling, and following Owen's (1964) results for $z_0' \approx u_*^2/g$, believes that the resulting Froude number,

$$z_0'/L \approx u_*^2/gL,$$

is the most important modeling parameter. It is the author's experience, gained using particles of various densities, that the equivalent roughness height z_0' is affected by density ratio ρ_p/ρ and that parameter 19 is thus more appropriate.

For modeling the gross features of full-scale snow-drifts, the mass transport rate parameter number 20 appears to be the most important. The value of the transport rate is significantly affected, however, as shown below, by changes in the value of roughness parameter 19. Parameters 17 and 18, derived from the particle equations of motion, appear to be important only in determining the characteristics of small-scale surface features (ripples) and thus can be ignored unless the small-scale features begin significantly to affect gross drift formation geometry.

In the study of grade-separation snow-drift problems two models were tested, one with a vertical geometric distortion in order to assist in ascertaining the effect of parameter 19. Thus, allowing for the possibility of vertical geometric distortion and using Jensen's criterion (Jensen, 1958; Cermak, 1975) for normal roughness modeling, the similitude problem becomes, for example (parameters 5, 6, 8, 13, 19, 20),

$$\frac{d(A/L^2)}{d(u_*t/L)} = \frac{\rho \, u_*^2}{\rho_p \, gH}\left(1 - \frac{u_*t}{u_*}\right) f\left\{A_1^2 \frac{D_p}{H}\left(\frac{u_*}{u_*t}\right)^2, \frac{u(H)\,L}{\nu}, \frac{h}{H}, \frac{l}{L}, \frac{z_0}{H}, \frac{H}{L}\right\} . \quad (1)$$

The Reynolds-number requirement, for relatively unstreamlined or rough-surface models, is usually specified as a minimum requirement; i.e. the model Reynolds number must exceed a minimum value, above which changes with Reynolds number are small (Cermak, 1975; Iversen, 1976).

TOPOGRAPHIC AND PARTICLE MODELS

Two models of the highway grade-separation structure were constructed. Model 1 was built at a 1 : 120 scale and Model 2 was built at the same scale horizontally but with a 1 : 60 scale in the vertical direction. Both models were covered with cloth to simulate grass except for the highway lanes which were smooth plastic (Ring and others, 1979). Three particles were selected for simulation of snow (Iversen, unpublished): 269 μm walnut shell (1 100 kg/m³), 101 μm glass spheres (2 500 kg/m³), and 49 μm dense glass spheres (3 990 kg/m³).

The models were placed at various orientations to the wind in a boundary-layer wind tunnel (1.2 × 1.2 × 7 m³ test section). The boundary layer depth at the model location (5 m down-wind) was increased to 0.25 m by turbulence-generating spires placed at the test section entrance. Particle material was placed to a uniform depth of 0.015 m (0.03 m for Model 2) across the test section width from 2.3 to 3.7 m down-wind of the test section entrance prior to the start of each experiment. Plan-view photographs of the model were taken at recorded times during each test run in order to measure the planform drift area on each stretch of highway lane as a function of time.

BARE-MODEL CALIBRATION

Both the undistorted and vertically-distorted grade-separation models were tested without simulated drift-control vegetation not only in order to obtain comparison with control planting configurations but also to obtain appropriate similitude relationships for more exact configuration comparisons and for possible extrapolation to full scale. With the wind direction parallel to the bridge center line, a total of 13 bare (simulated grass only) model experiments
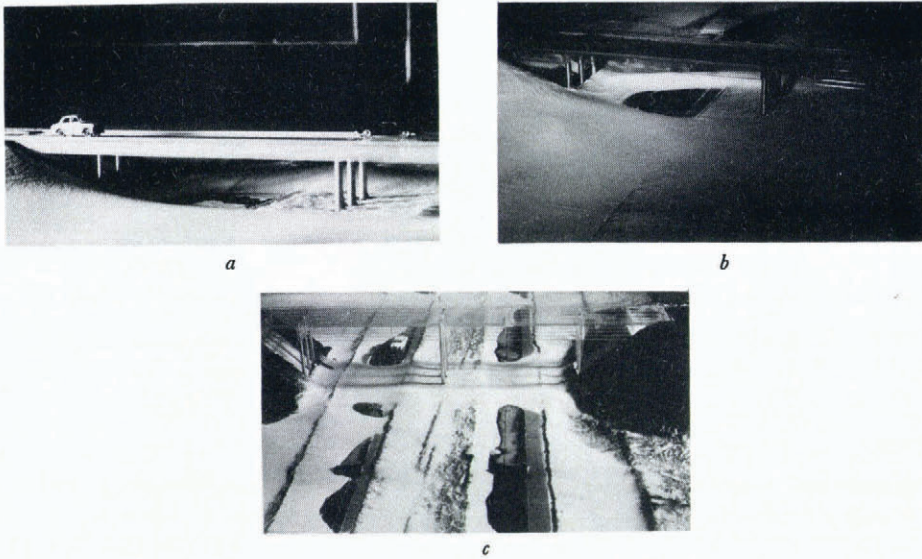
Fig. 1. *Photographs of bare (grass only) model calibration experiments. Scale-model cars were added after experiment was completed.*

   a. Run No. 2-24-1, wind direction left to right at 40° to bridge center line. Model 1.
   b. Run No. 12-7-1, wind direction left to right at 20° to bridge center line. Model 1.
   c. Run No. 3-27-1, wind direction left to right at 0° to bridge center line. Model 2.

were analyzed to produce the relationship desired. Ten of these experiments were with the undistorted model (Model 1) and three with the distorted model (Model 2). Photographs of some of these experiments are shown in Figure 1. Two experiments were with the 268 μm shell particles, three were with the 101 μm light glass, and the other eight were with the 49 μm dense glass. The 49 μm dense glass was used for all the remaining drift-control experiments. The planform drift area A divided by L^2 (bridge length squared) is shown for the 13 experiments as a function of dimensionless time in Figure 2.

RUN NUMBER	SPEED AT BRIDGE HEIGHT (m/s)	DENSITY RATIO ρ_p/ρ	PARTICLE DIAMETER $D_p/(\mu m)$	MODEL NUMBER
○ 10-19-1	4.96	900	269	1
□ 10-18-3	5.24	918	269	1
◁ 10-12-2	5.49	2081	101	1
◇ 10-12-1	5.69	2108	101	1
△ 10-12-3	6.44	2081	101	1
● 11-16-1	4.23	3225	49	1
■ 11-13-1	4.95	3350	49	1
▲ 10-17-2	5.61	3293	49	1
◆ 10-17-1	5.76	3238	49	1
◤ 11-7-1	6.70	3293	49	1
◁ 3-24-1	5.15	3159	49	2
◢ 3-27-1	5.45	3108	49	2
△ 3-26-1	6.12	3159	49	2
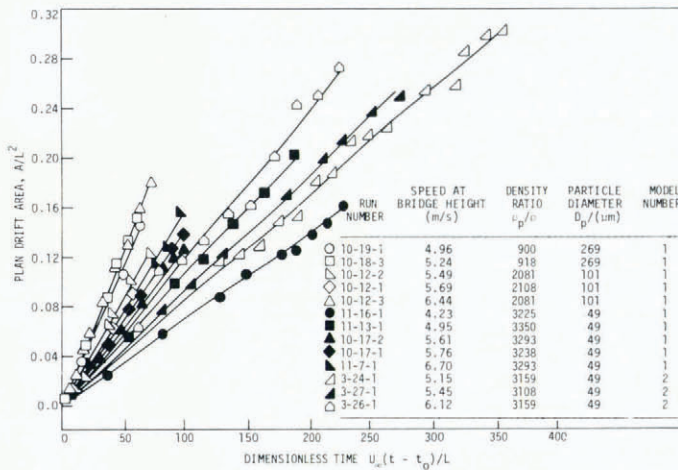
Fig. 2. *Plan-view drift area on interstate highway lanes as a function of time from the start of drifting. Speed ranges from 4.23 m/s to 6.70 m/s at 0° wind direction. Particle density ranges from 1 100 to 3 990 kg/m³ and particle diameter from 49 to 269 μm.*

TABLE II. VALUES OF MODELING PARAMETERS FROM CALIBRATION TESTS

	Range of model values				
	Model 1			Model 2	Range of full-scale values
Parameter	Shell	Light glass	Dense glass	Dense glass	
$C_D \rho L / \rho_p D_p$ [17]	7.6–7.7	28.1–28.7	113–125	115–117	27 000
gL^2/U^2H [18]	4.4–5.0	2.9–4.0	2.7–6.8	1.6–2.3	21–76
$A_1^2 \dfrac{D_p}{H}\left(\dfrac{u_*}{u_{*t}}\right)^2$ [19]	$(7.1$–$7.8) \times 10^{-4}$	$(3.8$–$5.2) \times 10^{-4}$	$(1.5$–$3.5) \times 10^{-4}$	$(0.95$–$1.3) \times 10^{-4}$	$(0.30$–$1.1) \times 10^{-4}$
$\dfrac{d(A/L^2)}{d(Ut/L)}\Big/\left\{\dfrac{\rho}{\rho_p}\dfrac{U^2}{2gH}\left(1-\dfrac{U_0}{U_\infty}\right)\right\}$ [20]	$(1.9$–$2.0) \times 10^{-3}$	$(2.4$–$2.9) \times 10^{-3}$	$(2.5$–$3.7) \times 10^{-3}$	$(4.5$–$5.0) \times 10^{-3}$	$(4.0$–$8.0) \times 10^{-3}$

The range of values of the four modeling parameters in the 13 bare model tests together with the corresponding full-scale values are depicted in Table II. The values of area A correspond to the snow-drift area (in plan) covering a 42 inch (105 cm) length of both lanes of highway including the shoulders. Obviously, the first two parameters are not modeled. These two parameters are of primary importance only if small-scale surface forms, such as ripples, are to be modeled to scale. Because of the use of the distorted model, the values of the third and fourth parameters, namely the roughness and mass-rate parameters, overlap the corresponding full-scale values giving more confidence in the results of the scale-model tests, since the third and fourth parameters are by far the most important in determining the gross drifting features and drift accumulation-rate.

The dimensionless rates of change of drift area for the bare model experiments were calculated using parameter 20. The results are shown in Figure 3 with the values of the mass transport rate parameter 20 plotted versus the saltation roughness parameter 19. The trend of decrease in the mass-rate parameter with increase in roughness is clear. In the absence of some theoretical relationship, a simple power-law equation was fitted to these data with the result as shown on the Figure. The full-scale values of roughness parameter are just to the left of
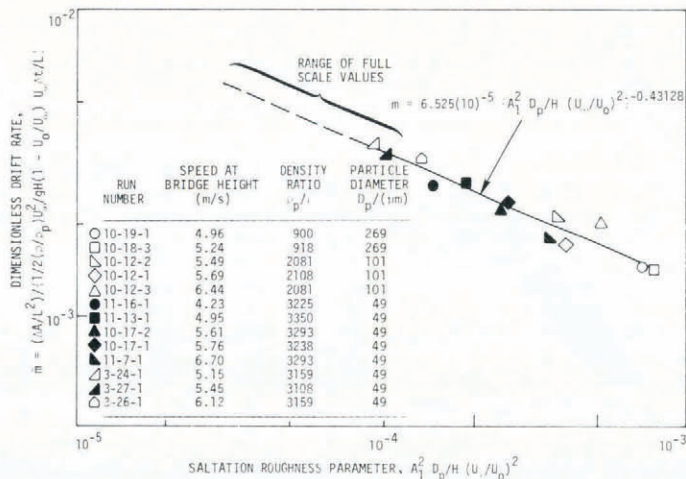
Fig. 3. Dimensionless drift rate using mass-rate parameter 20 versus roughness parameter 19. Same experiments as in Fig. 2.

most of the model values. It could thus be expected that the full-scale dimensionless drift rate (parameter 20) would be relatively somewhat larger than the model values. The dimensionless planform drift area is plotted against the combined mass-rate–roughness parameter in Figure 4. The correlation is quite good with the correlation coefficient $r = 0.9918$ ($r = \pm 1$ is a perfect correlation; r = slope multiplied by the ratio of horizontal and vertical standard deviations).
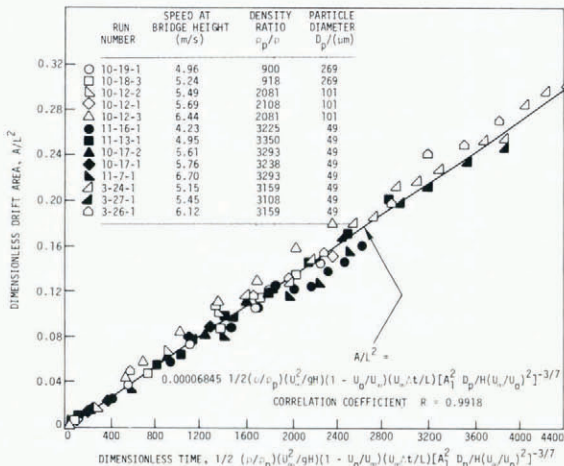
Fig. 4. *Dimensionless drift area versus combined mass-rate–roughness parameter. Same experiments as Figs 2 and 3.*

In order to evaluate the propriety of the various similitude parameters that other investigators have used or could possibly have used in comparison with the current mass-rate–roughness function, an attempt was made to correlate the dimensionless rate of change of area $d(A/L^2)/d(U_\infty \Delta t/L)$ as a function of several parameter possibilities. The results are found in detail in Ring and others (1979). The following equations with the corresponding correlation coefficients summarize the results:

$$d(A/L^2)/d(U_\infty t/L) \approx (U_\infty^2/gH)^{0.8} \qquad (r = 0.706), \qquad (2)$$

$$d(A/L^2)/d(U_\infty t/L) \approx (\rho U_\infty^2/\rho_p gH)^{0.63} \qquad (r = 0.956), \qquad (3)$$

$$d(A/L^2)/d(U_\infty t/L) \approx (\rho U_\infty^2(1 - U_0/U_\infty)/\rho_p gH)^{0.59} \qquad (r = 0.973), \qquad (4)$$

$$d(A/L^2)/d(U_\infty t/L) \approx \left[\frac{\rho}{\rho_p} \frac{U_\infty^2}{gH} \left(1 - \frac{U_0}{U_\infty} \right) \middle/ \left(A_1^2 \frac{D_p}{H} \left(\frac{U_\infty}{U_0} \right)^2 \right)^{3/7} \right] \qquad (r = 0.983). \qquad (5)$$

The correlation using the Froude number U_∞^2/gH is not valid with a correlation coefficient of only 0.706 for Equation (2). Equation (3), which is equivalent to using Bagnold's expression for the mass-rate equation and which takes the density ratio ρ/ρ_p into account, results in a considerable improvement and a relatively good correlation. Calkins (1975) indicated that $\rho U^2/\rho_p gL$ was an appropriate similitude parameter although he did not explain why he thought so. Calkins went on to abandon this parameter (which he labeled the densimetric Froude number) because full-scale projected speeds are unrealistic when using water as a model fluid. Use of the modified mass-transport rate (used to derive parameter 20) improves the correlation as in Equation (4), and addition of the roughness parameter (parameter 19) as in Equation (5) results in the best correlation coefficient. Kind's (1976) and Kawamura's (1951) expressions for mass-transport rate resulted in values of r of 0.93 and 0.96, respectively, which are not as good as those for Equation (4), but still represent reasonably acceptable values of correlation coefficient.
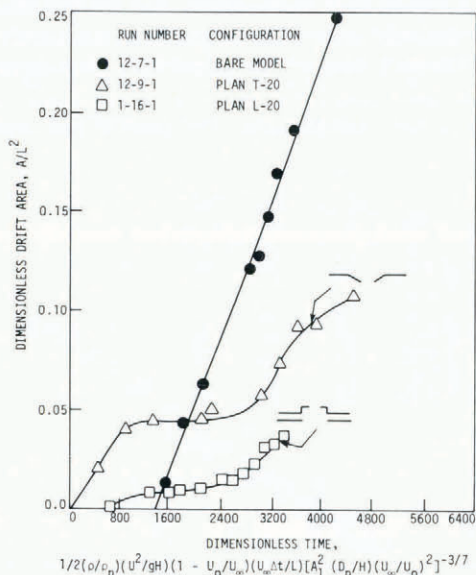
Fig. 5. *Dimensionless drift area versus combined mass-rate–roughness parameter. Wind direction 20° to bridge center line. Comparison of uncontrolled (bare model) and two different plan snow-drift control configurations. Model 1.*

TESTING THE SIMULATED VEGETATIVE SNOW-DRIFT CONTROL

Simulated rows of bushes (3 m full-scale height) were placed on the grade-separation model to act as snow-drift control barriers. Fifty-one experiments were performed with a variety of control configurations and with wind-speed direction angles of 0°, 20°, and 40° to the bridge center line. Typical results are shown in Figures 5 and 6. Two control configurations, one of good and one of mediocre performance, are compared in Figure 5 with a bare-model calibration at a 20° wind direction angle. It is as easy to create a planting configuration that can be considerably worse than no control as to create one that is a considerable improvement, such as plan L-20. Photographs of another experiment at 40° wind direction are illustrated in Figure 6. Results of all simulated vegetation experiments are reported in Ring and others (1979).
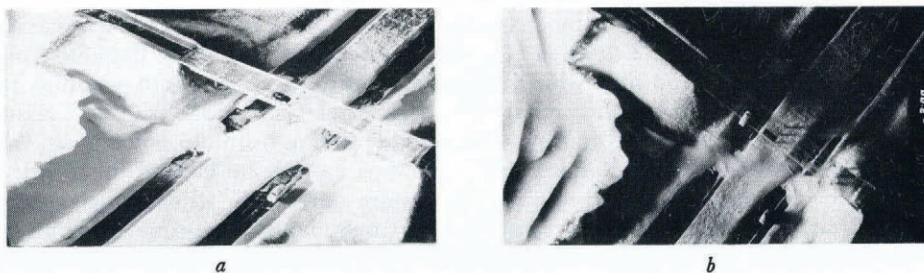
Fig. 6. *Photographs of Model 1 experiment (run 2-23-1) with wind direction from left to right at 40° to bridge center line. Scale-model cars were added after experiment was completed.*

a. Side view (approximately 45° from horizontal).
b. Plan view.

EFFECT OF VERTICAL DISTORTION

The results with the vertically distorted model (Model 2) at 0° wind direction for one bare-model experiment and one controlled-model experiment are shown in Figure 7 together with the corresponding results for the undistorted Model 1. The results for both configurations are displaced to the left for Model 2 compared with Model 1. The reason for this is that Model 2 is horizontally distorted as well as vertically distorted in conditions where there are separated flow or reduced-speed regions such as the lee side of the fill slope under the bridge and down-wind of the simulated plant control. The regions of reduced speed extend farther down-wind than in the undistorted Model 1 (or in full scale) because of the greater relative height of the fill slope and plant control in the distorted Model 2. Thus, early drifting occurs farther down-wind for Model 2 than for Model 1 and the drift area on the roadway is larger for corresponding times as shown in Figure 7. That Model 2 still gives valid relative results, at least for certain configurations, is shown by the fact that the two sets of curves are parallel and displaced vertically about the same distance. The curves would not be parallel without use of the combined parameter which includes the effect of roughness.
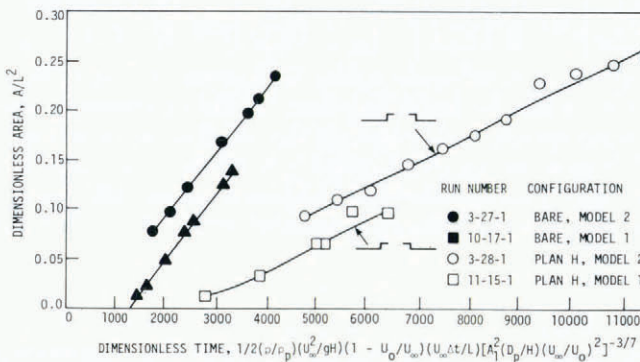
Fig. 7. Dimensionless drift area versus combined mass-rate–roughness parameter. Comparison of 0° wind-direction tests, controlled and uncontrolled, using Model 1 (true geometric model) and Model 2 (vertical geometric distortion factor of two).

EXTRAPOLATION OF MODEL RESULTS TO FULL SCALE

Previous investigators have usually used the Froude number U^2/gL as a means of determining the full-scale wind-speed and the duration of the modeled snow-storm time. This is believed to be incorrect as judged using the preceding similitude analysis and wind-tunnel test results. If, however, the Froude number is used (albeit incorrectly) as a means of extrapolation, then the full-scale–model wind-speed ratio U/U_m would just be the square root of the length ratio L/L_m. The time ratio $\Delta t/\Delta t_m$ would be the same value as the speed ratio. Using run number 10-17-1 as an example (model speed = 5.76 m/s and time duration = 18 minutes), the full-scale wind-speed would be 63.05 m/s (141 miles/h) and the duration would be 3 h 17 min, which are not very realistic values.

According to the wind-tunnel results of the 13 bare-model experiments, the appropriate extrapolation is to equate the combined mass-transport rate roughness parameters for model and full scale:

$$(\Delta A/L^2) \left[A_1{}^2 \frac{D_p}{H} \left(\frac{U}{U_0}\right)^2 \right]^{3/7} \Big/ \left\{ \frac{\rho}{\rho_p} \frac{U^2}{gH} \left(1 - \left(\frac{U_0}{U}\right)\right) \frac{U\Delta t}{L} \right\} \Big|_m$$

$$= (\Delta A/L^2) \left[A_1{}^2 \frac{D_p}{H} \left(\frac{U}{U_0}\right)^2 \right]^{3/7} \Big/ \left\{ \frac{\rho}{\rho_p} \frac{U^2}{gH} \left(1 - \left(\frac{U_0}{U}\right)\right) \frac{U\Delta t}{L} \right\} \Big|_f \quad (6)$$

It is assumed that everything is known in this equation except the full-scale values of U and Δt (or the model values of U and Δt which represent a given full-scale storm). Thus, another equation is needed in order to solve for the two unknowns of the second equation. One equation can be obtained by assuming that the ratio of particle speed to wind speed is the same in model and full scale. The second equation would then be

$$\left.\frac{U\Delta t}{L}\right|_{m} = \left.\frac{U\Delta t}{L}\right|_{f}. \tag{7}$$

For the example run 10-17-1, the values of full-scale wind-speed U and time duration Δt would be 14.68 m/s (32.8 miles/h) and 14 h 6 min, respectively.

The ratio of particle to wind-speed is not likely to be the same in full scale as in the model so it is probably more appropriate to search for another second equation. This can be done by equating the modified "densimetric Froude number", i.e.

$$\left.\frac{\rho}{\rho_p}\frac{U^2}{gH}\left(1 - \frac{U_0}{U}\right)\right|_{m} = \left.\frac{\rho}{\rho_p}\frac{U^2}{gH}\left(1 - \frac{U_0}{U}\right)\right|_{f}. \tag{8}$$

Then, in order to satisfy Equation (6),

$$\left.\frac{\Delta A}{UL\Delta t}\left[A_1{}^2\frac{D_p}{H}\left(\frac{U}{U_0}\right)^2\right]^{3/7}\right|_{m} = \left.\frac{\Delta A}{UL\Delta t}\left[A_1{}^2\frac{D_p}{H}\left(\frac{U}{U_0}\right)^2\right]^{3/7}\right|_{f}. \tag{9}$$

Equations (8) and (9) result in full-scale values for run 10-17-1 of 22.16 m/s (49.6 miles/h) for wind-speed and 5 h 32 min for storm duration. If the fundamental similitude Equation (6) is valid for all wind-speeds, then either of the wind-speed and time set of values of 14.68 m/s and 14 h 6 min or 22.16 m/s and 5 h 32 min are appropriate since both sets satisfy Equation (6). There probably are at least subtle differences with changes in wind-speed, however, and thus the latter set is probably more valid (based on the investigator's experience and intuition).

CONCLUSIONS

The dimensionless parameters derived by simple dimensional analysis for a given similitude problem can often be combined theoretically for modeling purposes. If not all original dimensionless parameters can be satisfied at model scale, then the model is distorted and some means of interpreting the effect of distortion must be determined. In the case of snow-drift modeling, it appears that the equivalent aerodynamic roughness height with material in motion derived by theoretical considerations of equivalent roughness is a significant distorted similitude parameter. The effect of varying the amount of roughness height distortion was determined by using particles of different diameter and density, different wind-tunnel speeds, and by testing a model with vertical geometric distortion as well as with a true geometric model.

The primary modeling parameter is considered to be the mass-rate parameter (parameter 20) which is derived from consideration of the amount of mass/unit time which can be transported by the wind. This parameter is combined empirically with the roughness parameter to correlate model-scale snow-drift accumulation data successfully as well as to predict equivalent full-scale wind-speeds and storm durations. The combined parameter has been used to compare a variety of drift-control techniques adjacent to an interstate highway grade-separation crossing.

REFERENCES

Bagnold, R. A. 1941. *The physics of blown sand and desert dunes*. London, Methuen and Co. Ltd.

Becker, A. 1944. Der natürliche Schneeschutz an Verkehrswegen. *Bautechnik*, 22. Jahrg., Ht. 37–42, p. 161–66.

Brier, F. W. 1972. *Snowdrift control techniques and procedures for polar facilities*. Port Hueneme, California, Naval Civil Engineering Laboratory. (Technical Report R767.)

Calkins, D. J. 1975. Simulated snowdrift patterns. *U.S. Cold Regions Research and Engineering Laboratory. Special Report* 219.

Cermak, J. E. 1975. Applications of fluid mechanics to wind engineering. *Journal of Fluids Engineering*, Ser. 1, Vol. 97, No. 1, p. 9–38.

de Krasinski, J. S., *and* Anson, W. A. 1975. A study of snowdrifts around the Canada Building in Calgary. *University of Calgary. Dept. of Mechanical Engineering. Report* No. 71.

Finney, E. A. 1934. Snow control on the highway. *Bulletin. Michigan Engineering Experiment Station* (East Lansing), No. 57.

Finney, E. A. 1937. Snow control by tree planting. Pt. VI. Wind tunnel experiments on tree plantings. *Bulletin. Michigan Engineering Experiment Station* (East Lansing), No. 75.

Finney, E. A. 1939. Snow drift control by highway design. *Bulletin. Michigan Engineering Experiment Station* (East Lansing), No. 86.

Gerdel, R. W., *and* Strom, G. H. 1961. Scale model simulation of a blowing snow environment. *Proceedings of the Institute of Environmental Sciences. National meeting, April 5, 6, 7 1961, Washington, D.C.*, p. 53–63.

Isyumov, N. Unpublished. An approach to the prediction of snow loads. [Ph.D. thesis, University of Western Ontario, 1971.]

Iversen, J. D. 1979. Drifting snow similitude. *Journal of the Hydraulics Division, American Society of Civil Engineers*, Vol. 105, No. HY6, p. 737–53.

Iversen, J. D. Unpublished. Drifting snow similitude—drift deposit rate correlation. [Paper presented at fifth International Conference on Wind Engineering, Colorado State University, Fort Collins, Colorado, 1979.]

Iversen, J. D., *and others*. 1973. Simulation of Martian eolian phenomena in the atmospheric wind tunnel, by J. D. Iversen, R. Greeley, J. B. Pollack, and B. R. White. (*In Space simulation. The proceedings of a symposium held November 12–14, 1973, at the International Hotel, Los Angeles, California*. Washington, D.C., Scientific and Technical Information Office, National Aeronautics and Space Administration, p. 191–213. (NASA SP-336.))

Iversen, J. D., *and others*. 1975. Eolian erosion on the Martian surface. Pt. 1. Erosion rate similitude, by J. D. Iversen, R. Greeley, B. R. White, and J. B. Pollack. *Icarus*, Vol. 26, No. 3, p. 321–31.

Iversen, J. D., *and others*. 1976. The effect of vertical distortion in the modeling of sedimentation phenomena: Martian crater wake streaks, by J. D. Iversen, R. Greeley, B. R. White, and J. B. Pollack. *Journal of Geophysical Research*, Vol. 81, No. 26, p. 4846–56.

Jensen, M. 1958. The model-law for phenomena in natural wind. *Ingeniøren*, C, Vol. 2, No. 4, p. 121–28.

Kawamura, R. 1951. Hisa no kenkyū [Study on sand movement by wind]. *Tōkyō Daigaku Rikōgaku Kenkyū Hōkoku*, [Vol.] 5, [Nos.] 3–4, p. 95–112.

Kind, R. J. 1976. A critical examination of the requirements for model simulation of wind-induced erosion/deposition phenomena such as snow drifting. *Atmospheric Environment*, Vol. 10, No. 3, p. 219–27.

Nøkkentved, C. 1940. Drivedannelse ved sneskærme. *Stads- og Havneingeniøren*, 31. Aarg., Nr. 9, p. 85–92.

Norem, H. 1974. *Utforming av veger i drivsnøomrader*. Trondheim, Institutt for Veg- og Jernbanebygging, Norges Tekniske Høgskole.

Odar, F. 1962. Scale factors for simulation of drifting snow. *Journal of the Engineering Mechanics Division, American Society of Civil Engineers*, Vol. 88, No. EM2, p. 1–16.

Odar, F. 1965. Simulation of drifting snow. *U.S. Cold Regions Research and Engineering Laboratory. Research Report* 174.

Owen, P. R. 1964. Saltation of uniform grains in air. *Journal of Fluid Mechanics*, Vol. 20, Pt. 2, p. 225–42.

Ring, S. R., *and others*. 1979. *Wind tunnel analysis of the effects of plantings at highway grade separation structures*, [by] S. R. Ring, J. D. Iversen, J. B. Sinatra, J. D. Benson. Ames, Iowa, Iowa State University in cooperation with the Highway Division, Iowa Dept. of Transportation. (Iowa Highway Research Board HR-202; ISU-ERI-Ames-79221, Project 1363.)

Strom, G. H., *and others*. 1962. Scale model studies on snow drifting, by G. H. Strom, G. R. Kelly, E. L. Deitz, and R. F. Weiss. *U.S. Snow, Ice and Permafrost Research Establishment. Research Report* 73.

Tabler, R. D. 1980. Self-similarity of wind profiles in blowing snow allows outdoor modeling. *Journal of Glaciology*, Vol. 26, No. 94, p. 421–34.

Theakston, F. A. 1970. Model technique for controlling snow on roads and runways. *U.S. Cold Regions Research and Engineering Laboratory. Special Report* 115, p. 226–30.

White, B. R., *and others*. 1976. Estimated grain saltation in a Martian atmosphere, by B. R. White, R. Greeley, J. D. Iversen, and J. B. Pollack. *Journal of Geophysical Research*, Vol. 81, No. 32, p. 5643–50.